Excitonic absorption of GaN epilayers on sapphire: Dynamics, intensity, and temperature dependence

H. Haag, P. Gilliot, R. Lévy, and B. Hönerlage
Groupe d'Optique Nonlinéaire et d'Optoélectronique, Institut de Physique et Chimie des Matériaux de Strasbourg, UMR 7504 CNRS-ULP, 23, Rue du Loess, Boîte Postale 20CR, F-67037 Strasbourg Cedex, France

O. Briot, S. Ruffenach-Clur, and R. L. Aulombard
Groupe d'Étude des Semiconducteurs, URA 357 CNRS, Université de Montpellier II, Place Eugène Bataillon, F-34095 Montpellier Cedex 05, France

(Received 21 April 1998; revised manuscript received 6 July 1998)

Using test-pump measurements, we studied the excitonic absorption of GaN epilayers on sapphire substrate under nanosecond and picosecond pulsed excitation conditions. We measured a short exciton lifetime of 25 ps, which is consistent with results obtained from degenerate four-wave mixing measurements. Since the radiative lifetime should be much longer, this short characteristic time shows the dominance of nonradiative processes. Under nonresonant excitation condition, we observed an intensity dependent shift and damping of the exciton resonance, attributed to an inhomogeneous temperature distribution. This thermal effect was not observed under resonant excitation conditions. This behavior is tentatively explained by the presence of shallow centers that have a rather long lifetime and recombine nonradiatively. [S0163-1829(99)10203-0]

I. INTRODUCTION

Gallium nitride is a direct-band-gap semiconductor having an energy gap of approximately 3.50 eV at liquid-helium temperature.[1] It is considered to be one of the most promising materials for the elaboration of light emitting devices in the blue-green spectral region.[2] For applications in optoelectronics, one has to search for a better understanding of energy relaxation and transport processes close to the exciton resonance of the material. In recent years, GaN films of good optical quality have been grown on sapphire substrate mainly by molecular-beam epitaxy (MBE) or by metal organic chemical vapor deposition (MOCVD). Although an important lattice mismatch between the sapphire substrate and GaN exists, a good optical quality was obtained when AlN or GaN buffer layers were first grown at low temperatures on the substrate,[3–6] which is annealed afterwards. In this way, it is possible to produce high-quality samples, which are thin enough to exhibit excitonic structures in their absorption spectra.[7] It has been shown that epitaxial layers of GaN (Refs. 8 and 9) or InGaN (Ref. 10) show strong nonlinearities near their absorption edge, but their origin is still not clear.

The sample studied throughout this work is an epilayer of unintentionally doped GaN, grown by MOCVD on a (0001) sapphire substrate with an intermediate AlN buffer. Because of the important exciton absorption ($\alpha \sim 10^6$ cm^{-1}) we were bound to investigate thin samples, which is quite problematic on two points. First, it has been shown that the quality of GaN samples increases with increasing thickness of the layer.[11,12] Additionally, it is well known that residual strain due to the lattice mismatch between substrate and sample modifies the electronic band structure of GaN.[13,14] This gives rise to a shift of the conduction band having Γ_7 symmetry. In addition, it affects the valence band by mixing the valence-band states and changing their energies with respect to the nonperturbed situation.

In this paper, we were mainly interested in the nonlinear absorption characteristics of GaN close to the excitonic resonance under high-excitation conditions. We first describe the experimental setup. Then, we study the linear properties in detail, in order to explain further results obtained by standard test-pump and four-wave mixing measurements in the nanosecond and picosecond regime.

II. EXPERIMENTAL SETUP

For low-temperature measurements, the sample is immersed in pumped liquid helium below the λ point, or in a continuous He flow cryostat if the temperature dependence of the transmission is studied. Linear reflection and transmission spectra are obtained with a high-pressure Xe lamp using lock-in techniques. The reflected or transmitted light is focused onto the entrance slit of a 65-cm Jobin-Yvon spectrometer and detected by a photomultiplier. The overall spectral resolution is better than 0.5 meV. To measure linear luminescence spectra, the sample is excited at $\hbar\omega_{\mathrm{exc}} = 4.024$ eV (308 nm) by the emission of a XeCl excimer laser delivering pulses of 20 ns with a repetition rate of 5 Hz. The excitation intensity is kept sufficiently low to avoid nonlinear processes ($I = 2$ kW cm^{-2}) as P lines, stimulated emission, or gain.[15–17]

We also used the excimer laser to perform pump and probe measurements at high intensities of excitation. In these experiments, probe pulses of approximately 7 ns duration are obtained from the superradiant emission of BMQ dye dissolved in dioxane, pumped by one part of the excimer laser emission. The pulses transmitted through the sample at liquid-He temperature (with or without excitation) are dispersed by a 75-cm Spex spectrograph, pass a light amplifier and are detected by a Reticon camera. The spectral resolution

 ©1999 The American Physical Society

is about 0.5 meV. The intensity dependence of the nonlinear transmission spectra was obtained either by exciting the sample with the excimer laser at 4.02 eV, or by a tuneable dye laser, pumped by the excimer laser. The intensity of pump pulses can be varied between 0 to 75 kW cm^{-2}. In the dye laser, having a grating working in grazing incidence, the active medium is also BMQ dissolved in dioxane.

The spectral width of the output pulses of 7 ns duration is less than 0.05 meV and the tuning range between 3.40 and 3.55 eV, thus covering the absorption region of *A, B*, and *C* excitons. For test-pump measurements under picosecond excitation conditions, we excite the sample by single pulses of the fourth harmonics of a Nd:-YAG laser (4.659 eV) with a repetition rate of 10 Hz. Probe pulses are obtained by the superradiant emission of a dye (BMQ in dioxane) excited by part of the pulses. The pulse duration of both beams is measured with a Streak camera and found to be about 25 ps. The time delay between pump and probe pulses is adjusted by using an optical delay on the probe pulse. The transmitted pulses are detected similarly as in the nanosecond setup (using a 65-cm Jobin-Yvon spectrograph) with a resolution of about 0.5 meV. In order to control the intensity fluctuations of the pump beam, pump pulse intensities are discriminated and only pump pulses within a window of ± 10 % around a mean value are considered when the signals are read out.

In standard degenerate four-wave mixing experiments,[18,19] two pulses at temporal coincidence excite the sample under different angles. They form an intensity grating, on which a time delayed third pulse is diffracted. The temporal behavior of the diffraction intensity gives a measure of the time evolution of the complex index of refraction which is, in our case, function of the exciton and/or electron-hole density. Pulses used for our measurements are generated by the third harmonics of a Nd-YAG laser (3.49 eV) delivering pulses of about 25 ps. The diffracted beam is detected by a Reticon camera and the signals are again selected in order to compensate the intensity fluctuations of the pump pulses.

III. LINEAR OPTICAL CHARACTERIZATION AND TEMPERATURE DEPENDENCE OF EXCITONIC RESONANCES

In optical experiments, transitions from all three valence bands to the conduction band of GaN are possible if the polarization vector of the light field **E** is perpendicular to the optical axis **c** of the sample.[20] This is the case for films grown on sapphire substrate where **c** is parallel to the growth direction, i.e., perpendicular to the plane of the substrate. Then, three exciton series may be observed in reflection and in absorption, corresponding to the $\Gamma_9^v - \Gamma_7^c$, $\Gamma_7^v - \Gamma_7^c$, and $\Gamma_7^v - \Gamma_7^c$ interband transitions, which are usually labeled *A, B*, and *C*, respectively. When using wave vectors $\mathbf{K} \| \mathbf{c}$ and adopting the polariton concept[21] due to the nonanalytic exchange interaction, dipole active excitons of Γ_2 and Γ_5 symmetry are further split into longitudinal and transverse exciton states with eigenfrequencies $\hbar\omega_L$ and $\hbar\omega_T$.

For linear optical characterization, the resulting measured luminescence intensity $I_L^M(\hbar\omega)$ is given in Fig. 1(b) by the thin line. Since in this spectral region the absorption coefficient [as can be determined from the absorption spectrum in

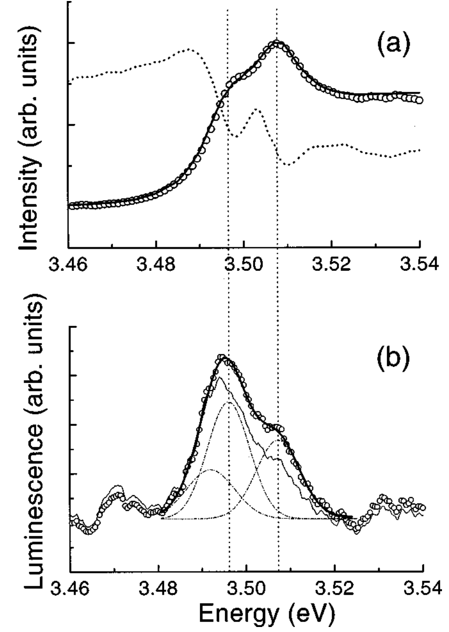

FIG. 1. (a) Measured linear reflection (dotted line) and absorption (open circles) spectra of a 0.35-μm-thick GaN film at 2 K and normal incidence. The fit of the absorption spectra obtained with Eq. (2) is shown by the full line. (b) Emission spectrum of the sample excited at 4.024 eV at low intensities (thin line). The luminescence is corrected for reabsorption (open circles) and deconvoluted (full line) into three Gaussian lines (dashed-dotted lines) as explained in the text.

Fig. 1(a)] is strongly dependent on the photon energy, we have to correct the luminescence spectra with respect to the reabsorption and to the inhomogeneous excitation by the excimer laser. Neglecting reflection losses in the corrected luminescence spectrum, $I_L^0(\hbar\omega)$ is then given by[22]

$$I_L^0(\hbar\omega) \propto \frac{I_L^M(\hbar\omega)[\alpha(\hbar\omega)+\alpha(\hbar\omega_{\rm ex})]d}{1-\exp\{-[\alpha(\hbar\omega)+\alpha(\hbar\omega_{\rm ex})]d\}}, \tag{1}$$

where $\alpha(\hbar\omega)$ is the photon-energy-dependent absorption coefficient governing the reabsorption, $\alpha(\hbar\omega_{\rm ex}) = 10^6$ cm^{-1} gives rise to the inhomogeneous excitation profile and $d = 0.35$ μm is the sample thickness. As we will see later, the exciton lifetime in our sample is very short (~20 ps), such that diffusion processes can be neglected, and the simple model of Eq. (1) applied. When comparing the different spectra of Fig. 1, one first clearly remarks two spectral resonances at 3.497 and 3.508 eV, which we attribute to the *A* and *B* excitons, respectively. As discussed in the introduction, these relatively high exciton energies are due to the important compressive strain present in the 0.35-μm-thick sample.[14] Concerning the *B* exciton, resonances of the absorption and luminescence spectra are (within our experimental precision) exactly at the same photon energy. Additionally, no phonon replicas are observed in the luminescence spectra. Therefore, we conclude that the coupling to longitudinal optical phonons having an energy of $\hbar\omega_{\rm LO} = 91.6$ meV (Refs. 23 and 24) is quite small.

Concerning the *A*-exciton emission and absorption, two problems arise: first, the spectral position of the *A* exciton cannot be determined with the same precision from the ab-

sorption spectrum as it is the case for the B exciton. The maximum of the exciton luminescence, on the contrary, is situated at 3.494 eV and shows a shoulder around 3.491 eV. This shoulder is probably due to the well-known emission from an exciton bound to a neutral donor (D^0X complex), situated 5.8 meV below the A exciton resonance.[25] We therefore deconvolute the exciton emission into three lines of Gaussian shape at 3.491, 3.497, and 3.508 eV corresponding to the D^0X-, A-, and B-exciton lines, respectively. They are given in Fig. 1(b) by the dashed-dotted lines and their sum by the full line. We clearly see that the emission is dominated by free A- and B-exciton emission and that the D^0X-exciton emission gives rise only to a minor contribution at 2 K.[26] We can now fit the absorption spectra [Fig. 1(a)] with Eliott's theory,[27] assuming three excitonic resonances corresponding to the A, B, and C excitons in the $1s$ state:

$$\alpha(\omega)\propto\sum_{i=A,B,C}4\pi f_i\delta(\Delta+1)+\theta(\Delta)\,\frac{\pi e^{\omega/\Delta}}{sh(\pi/\Delta)},\qquad(2)$$

where $\Delta=(2\hbar^2\varepsilon_0^2/e^4\mu)(\hbar\omega-E_g)$, $\delta(x)=1/[\pi\Gamma ch(x/\Gamma)]$, $\theta(x)$ is the Heavyside unit-step function, E_g is the energy gap, f_i the oscillator strength, μ the reduced mass ($\mu=0.15m_0$, assumed to be the same for all excitons) and Γ the linewidth of the excitonic resonances. Spectral positions of the A and B excitons are determined by the luminescence spectra and fixed to 3.497 and 3.508 eV, respectively. In addition, the small luminescence maximum at 3.532 eV is tentatively attributed to the C-exciton emission. The best fit of Eq. (2) is obtained with the following values: $E_g=3.557$ eV, $f_A=0.26$, $f_B=0.33$, $f_C=0.13$, and $\Gamma=7.32$ meV.

Let us now compare these results with the reflection spectrum. We find well-pronounced minima of reflection at 3.510 and 3.499 eV. Usually, at normal incidence, reflection minima are very close to the energy of the longitudinal exciton $\hbar\omega_L$ and (due to the high density of states in the polariton model) absorption maxima are close to that of the transverse excitons[28] $\hbar\omega_T$. This statement remains valid even if spatial dispersion and exciton free layers have to be included into the interpretation of reflection spectra.[29] Therefore, we conclude that the oscillator strength (proportional to the longitudinal-transverse splitting $\Delta_{\rm LT}=2$ meV in the case of the B exciton) of both A and B excitons are comparable, in agreement with the values obtained from Eq. (2). Again, the small reflection structure around 3.532 eV is attributed to the C exciton.[30]

The damping constant Γ obtained from the fit of the absorption measurements and the linewidth of the luminescence both largely exceed the longitudinal-transverse splitting $\Delta_{\rm LT}$ of the exciton resonances. This indicates that both resonances are probably not due to free-exciton lines, which are homogeneously broadened due to the finite coherence time of the states, but rather due to exciton lines that are inhomogeneously broadened due to exciton localization or to the strain which varies with the film depth. Γ and the deconvolution of the luminescence spectrum then rather reflect the distribution of the states in these bands. This interpretation is in agreement with Ref. 31, where the homogeneous exciton line of about 1.7 meV has been reported for a 3-μm-thick sample.[31] Inhomogeneous broadening, of course, smears out the reflection structures discussed above but our argument concerning the spectral position of the reflection minima and absorption maxima should remain valid. The rather close coincidence of reflection minima and absorption maxima could also result from the aforementioned inhomogeneous strain, which is probed by different methods at different depths of the sample.

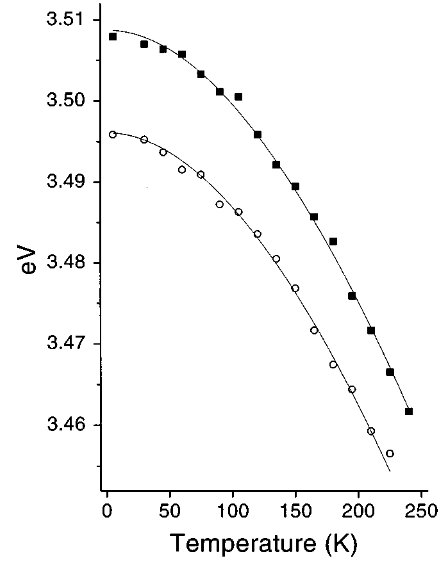

FIG. 2. Temperature variation of the A- and B-exciton resonance (open circles and full squares, respectively). Full lines are calculated with Varshni's formula and the parameters given in the text.

In order to determine the exciton-phonon interaction, we measured the absorption spectra of our sample for different temperatures. It is important to notice that the absorption of the A and the B excitons remain well defined up to about 150 K, i.e., the half-width of the absorption line approximately doubles when heating the sample from 2 to 150 K. From this measurements, we determine the spectral positions of the A and B transverse excitons as a function of the temperature, which follow the energy gap. It appears in Fig. 2 that their separation remains constant at 11 meV and the energy gap shrinks by about 45 meV when the temperature increases from 2 to 240 K. As shown by the full lines in Fig. 2, the variation of the exciton energy as a function of the temperature of the sample follows the phenomenological Varshni formula[32]

$$E(T)=E_0-\alpha T^2/(T+\beta),\qquad(3)$$

where $\alpha=10^{-3}$ eV K^{-1}, $\beta=1000$ K, are constants and E_0 is the energy of the A and B excitons, respectively, at $T=0$ K. The values of α and β are not very precise but give only an order of magnitude.

Using Eq. (2), we can determine the variation of the excitonic linewidth Γ as a function of the lattice temperature. By increasing the lattice temperature, Γ stays constant at 7.5 meV up to 40 K and then increases linearly, in order to reach 20 meV at 200 K. We can fit $\Gamma(T)$ with the following phenomenological equation:[33]

$$\Gamma(T)=\Gamma_0+aT+bn(T),\qquad(4)$$

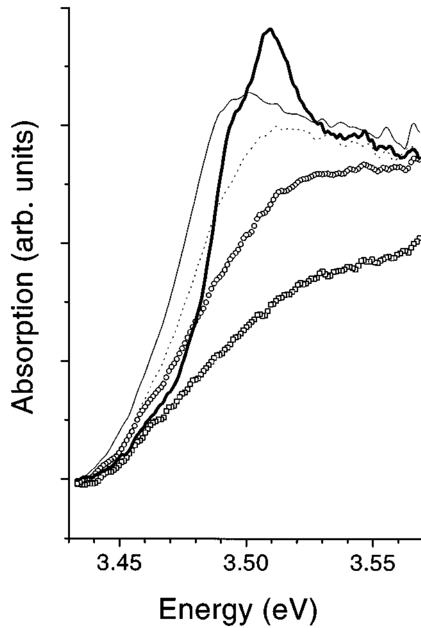

FIG. 3. Absorption spectra for different delays t between test and pump pulses of $I_{ex}=87$ kW cm^{-2} (squares $t=0$ ps; circles, $t=25$ ps; dots, $t=40$ ps; line, $t=1.5$ ns; bold line, linear absorption).

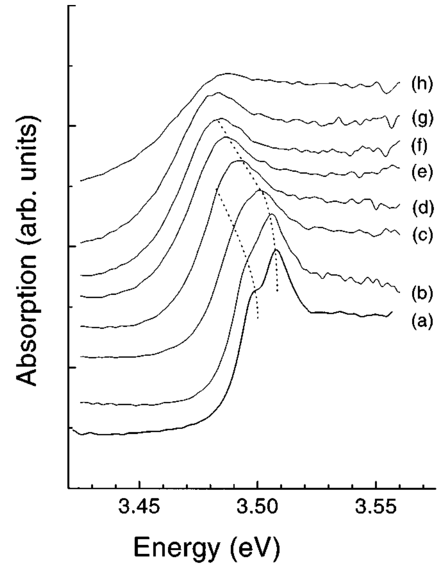

FIG. 4. Absorption spectra at 2 K when the sample is excited at 4.024 eV with nanosecond pulses of different intensities (a) 0 kW cm^{-2}, (b) 8 kW cm^{-2}, (c) 14 kW cm^{-2}, (d) 24 kW cm^{-2}, (e) 38 kW cm^{-2}, (f) 46 kW cm^{-2}, (g) 58 kW cm^{-2}, (h) 75 kW cm^{-2}.

where Γ_0 is a temperature independent term due to the inhomogeneous broadening, aT is the contribution of acoustic phonons, and $bn(T)$ reflects the scattering with optical phonons which have an occupation factor $n(T) = 1/[\exp(\hbar\omega_{LO}/kT)-1]$. The best fit is obtained with $\Gamma_0 = 7.3$ meV, $a=7$ μeV K^{-1}, and $b=137$ meV.

To conclude this part, it is important to stress that the exciton energies given in this paper were obtained with a 0.35-μm-thick film that contains considerable residual strain. For this reason, the energy of the A exciton in our sample is $\hbar\omega_T(A)=3.496$ eV, which is about 25 meV higher than in an unstrained one.[13] The presence of exciton resonances that dominate our absorption, reflection or luminescence spectra shows, however, that our samples are of quite good optical quality.

IV. THERMAL EFFECTS ON THE EXCITONIC ABSORPTION AT HIGH EXCITATION INTENSITY

A. Nonlinear transmission spectra under nanosecond and picosecond excitation conditions

For test-pump measurements under picosecond excitation conditions, we excite the sample at 4.659 eV for a fixed excitation intensity of 87 kW cm^{-2}. The absorption spectrum is determined for different time delays between test and pump pulses (Fig. 3). At temporal coincidence, band filling effects first show up, leading to the quenching of the excitonic resonances. After excitation, a rapid decay is observed, characteristic for the time restitution of the excitonic resonances. Then, at delays of approximately 40 ps after the excitation, the excitonic resonances show up again but shifted by about 8 meV to lower energies. The excitonic resonance remains at this spectral position, indicating a relaxation time longer than 10 ns. As we will discuss later, we attribute this redshift of 8 meV to a heating of the sample, induced by the pump pulses. The long time constant of 10 ns indicates the bad thermal conductivity of the film, since the sample is immersed in liquid He and the sapphire substrate has a very high thermal conductivity at 2 K.

This thermal behavior also appears by measuring the intensity dependence of the absorption spectrum under nanosecond excitation conditions. We present in Fig. 4 the variation of the absorption spectra for different intensities of pump pulses, exciting the sample at a photon energy of $\hbar\omega_{ex}=4.024$ eV. Our maximum excitation intensity of 75 kW cm^{-2} leads to a density of electron-hole pairs of the order of 9×10^{18} cm^{-3} (obtained with a carrier lifetime of 20 ps and an optical density of 0.8). This value is higher than the Mott density of 6×10^{18} cm^{-3}, which can be obtained experimentally with pulses of 50 kW cm^{-2}. Due to the excitation, one clearly observes Fig. 4 an overall decrease of the sample absorption, accompanied with a spectral shift of both exciton resonances to lower energies. Since we attribute this effect to a heating of the sample, we compare Fig. 4 to linear absorption spectra for different temperatures (Fig. 2). We find that the excitation leads to an increase of temperature of approximately 130 K when exciting with an intensity of 46 kW cm^{-2}. In addition, the absorption spectra with pump excitation (Fig. 4) show that the A-exciton absorption becomes more important than that of the B exciton with increasing intensity. In addition, absorption and reflection structures under high intensities of excitation are broader than linear structures, which may be due to an increase of the exciton damping due to scattering processes with free carriers, or simply to an inhomogeneous temperature profile.

We show Fig. 5 resonant exciton excitation experiments at 2 K, using a constant excitation intensity of 72 kW cm^{-2}. The excitonic resonances A and B are smeared out and the overall absorption decreases drastically when the photon energy of the pump beam is tuned into the exciton resonance. Contrary to the band to band excitation as function of inten-

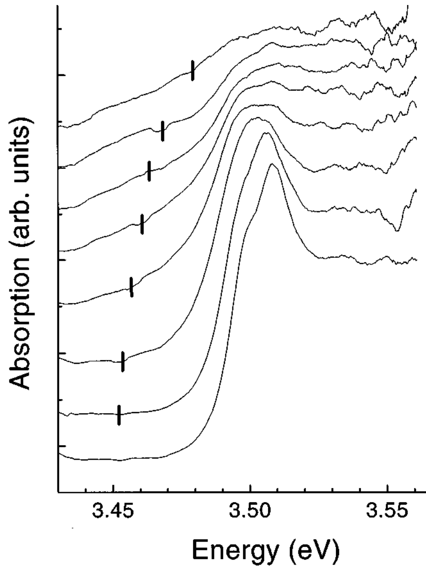

FIG. 5. Absorption spectra of GaN at 2 K when excited at different photon energies by a dye laser at excitation intensity of 75 kW cm^{-2}. Its photon energy is indicated by vertical bold lines.

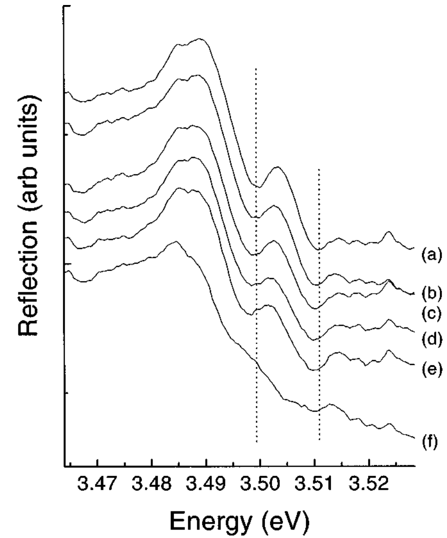

FIG. 6. Reflection spectra at 2 K when the sample is excited at 4.024 eV with nanosecond pulses for different intensities (a) $=0$ kW cm^{-2}, (b) $=5$ kW cm^{-2}, (c) $=11$ kW cm^{-2}, (d) $=24$ kW cm^{-2}, (e) $=42$ kW cm^{-2}, and (f) $=61$ kW cm^{-2}.

sity, thermal effects are only slightly observed here. In the same way, no heating has been observed by time resolved pump and probe experiments performed under resonant excitation ($\hbar\omega_p=3.49$ eV) in the picosecond regime. In this case, the transmission decreases under excitation and returns to its initial value with a time constant of about 25 ps. We explain these results by the fact that under resonant excitation of the excitons, nonradiative recombination processes leading to a heating of the sample are less important than band filling effects, band-gap renormalization, or Coulomb screening (see Sec. V C). Band filling effects are predominantly responsible to an increase of the exciton damping due to collision processes between excitons or with the electron-hole plasma. In addition, collision processes give rise to an important exciton population in the bottleneck region and may lead to an important induced absorption. Such effects have been clearly observed in emission spectroscopy.[21,34] Therefore, we suppose that thermal effects are essentially due to thermalization of carriers in the continuum states.

B. Nonlinear reflection spectra under nanosecond excitation

Figure 6 shows the variation of the nonlinear reflection spectra for different intensities of a pump beam, exciting the sample at 4.02 eV. It appears that the shift of the exciton resonances is much smaller in reflection than in absorption under the same excitation conditions. This shift corresponds to a maximum induced temperature change at the surface of the sample of 30 K. To explain this inhomogeneous temperature profile between surface and bulk measurements, we remind that our sample is immersed into a bath of liquid helium pumped below the λ point. Therefore, rapid heat exchange takes place on the surface of the sample. On the other hand, a slow heat diffusion due to the bad thermal conductivity of GaN would explain the higher temperature of the core of the sample (tested in a transmission configuration), and the inhomogeneous heat profile that smears out the exciton resonances in transmission measurements under high excitation conditions.

V. EXCITON DYNAMICS UNDER PICOSECOND EXCITATION CONDITIONS

A. Pump and probe experiments

From the pump and probe experiments performed under picosecond excitation (Fig. 3), we determine the absorption change as a function of the time delay. This is shown in Fig. 7 for an excitation intensity of $I_{ex}=87$ kW cm^{-2}. The photon energy is fixed at $\hbar\omega=3.508$ eV, which corresponds to the energy of the B exciton at 2 K. Since the measured characteristic time is close to our experimental resolution, we fit our data assuming that the carriers are generated by a pulse with a Gaussian shape and decay exponentially:

$$\frac{dn(t)}{dt}=G(t)-\frac{1}{\tau}n(t), \tag{5}$$

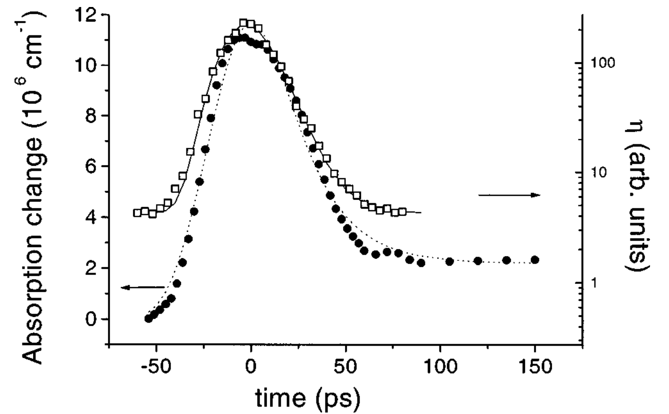

FIG. 7. Excitonic recombination under picosecond regime: dynamics of the excitonic absorption ($\hbar\omega_T=3.508$ eV) under non-resonant excitation condition ($\hbar\omega_P=4.66$ eV) for $I_{ex}=87$ kW cm^{-2} [full circles, data; dotted line, fit with Eq. (5)] and temporal behavior of the diffraction efficiency obtained by FWM measurements under resonant excitation condition ($\hbar\omega_P=4.66$ eV) for $I_{ex}=75$ kW cm^{-2} [open squares, experimental data; line, fit with Eq. (7)].

where $n(t)$ is the density of carriers, $G(t)=G_0 e^{-t^2/\sigma}$ is the generation rate of width σ, and τ is the characteristic time of decay. We suppress the constant absorption change and deconvolute the absorption change $\delta(t)$ with the test pulse:

$$\delta(t)=\int n(t)G(t-t')dt'. \quad (6)$$

We find a characteristic time of 23 ps, which is independent of the lattice temperature of the sample.

B. Four-wave mixing experiments

As shown in Fig. 7, the temporal evolution of test-pump measurements is comparable to the results obtained in standard degenerate four-wave mixing experiments. We notice that pump pulses excite the sample at 3.49 eV, i.e., close to the excitonic resonances. Since there is no excess of energy from the exciting pulses, no thermal effects are expected in this experiment.

Again, the time constants obtained are very close to our experimental resolution. We fit our data by the same model as for the test-pump measurements [Eq. (5)] and deconvolute the diffraction efficiency $\eta(t)$ by the test pulse:

$$\eta(t)=\int_{-\infty}^{\infty} n^2(t)G(t-t')dt'. \quad (7)$$

In agreement with pump and probe experiments, we find decay times of about 20 ps, which is independent of the lattice temperature and of the fringe spacing of the grating. This latter means that diffusion does not show up during the short lifetime of the free carriers. In addition, the relaxation time τ depends slightly on the excitation intensity, indicating the importance of bimolecular electron-hole recombination, exciton/exciton scattering, or Auger recombination processes. Time-resolved luminescence measurements on the sample also exhibit the same temporal behavior.

C. Discussion

Theoretically, energy relaxation times of the order of several nanoseconds are expected for good monocrystalline GaN/films.[35] Indeed, thicker samples (which have a better crystalline structure) exhibit excitonic decay times up to 500 ps.[36] On the other hand, very short energy relaxation times have been observed in test-pump and four-wave mixing experiments performed on polycrystalline CdZnTe (Refs. 37 and 38) or porous silicon.[39] Therefore, we attribute the fast energy relaxation time to structural defects of our sample, which lead to an important nonradiative channel.

Important nonradiative recombinations should strongly heat the sample, which was not observed under resonant excitation conditions, neither in the nanosecond nor in the picosecond regime. In addition, test-pump experiments have been performed on a GaN sample by Shan *et al.*[5] under resonant excitation conditions but, as in our case, heating processes were not observed. This can be tentatively explained by the presence of shallow centers. Trapped carriers should recombine nonradiatively with a long characteristic time, thus masking thermal effects.[40]

VI. CONCLUSION

We have shown that exciton localization, rapid electronic effects, and sample heating govern the scenario of optical nonlinearities and energy relaxation of 0.35-μm-thick GaN films at 2 K. Under nanosecond pulsed band to band excitations, pump and probe experiments show a redshift of the excitonic resonances, which is interpreted by a heating of the sample induced by the pump beam. This is confirmed by time-resolved experiments in the picosecond regime: the redshift appears roughly 40 ps after the pulse excitation and decreases with a characteristic time of the order of several nanoseconds. This heating does not occur under resonant excitation conditions. The difference between nonlinear absorption and reflection spectra is explained by the low thermal conductivity of GaN, which leads to an inhomogeneous temperature profile within the sample. Since the coupling to optical phonons is quite small, the rapid energy relaxation time of 20 ps measured by time-resolved test-pump experiments is attributed to a high density of crystal defects, which gives rise to such short lifetimes. Degenerate four-wave mixing experiments confirm the temporal behavior of the excited states and show no diffusion of carriers.

Even if nonradiative recombination is important, pump and probe and DFWM experiments under resonant excitation conditions have shown that they have no influence on thermal processes. This is assumed to be due to the presence of shallow centers responsible for the nonradiative path. Trapped carriers relax nonradiatively with a long characteristic time.

[1] B. Monemar, Phys. Rev. B **10**, 676 (1974).
[2] P. Rigby, Nature (London) **384**, 610 (1996).
[3] H. Amano, M. Kito, K. Hiramatsu, and I. Akasaki, Jpn. J. Appl. Phys., Part 1 **28**, L2112 (1989).
[4] S. Nakamura, T. Mukai, and M. Senoh, Appl. Phys. Lett. **64**, 1687 (1994).
[5] W. Shan, T. J. Schmidt, X. H. Yang, S. J. Hwang, J. J. Song, and B. Goldenberg, Appl. Phys. Lett. **66**, 985 (1995).
[6] F. A. Ponce, D. P. Bour, W. Götz, N. M. Johnson, H. I. Helava, I. Grzegory, J. Jun, and S. Porowski, Appl. Phys. Lett. **68**, 957 (1996).
[7] B. Thaeri, J. Hays, J. J. Song, and B. Goldenberg, Appl. Phys. Lett. **68**, 587 (1996).
[8] T. J. Schmidt, J. J. Song, Y. C. Chang, R. Horning, and B. Goldenberg, Appl. Phys. Lett. **72**, 1504 (1998).
[9] A. Hoffmann, Adv. Solid State Phys. **36**, 33 (1997).
[10] C. K. Sun, F. Vallée, S. Keller, J. E. Bowers, and S. B. DenBaars, Appl. Phys. Lett. **70**, 2004 (1997).
[11] C. Kim, I. K. Robinson, J. Myoung, K. Shim, M-C. Yoo, and K. Kim, Appl. Phys. Lett. **69**, 2358 (1996).
[12] H. Siegle, P. Thuriam, L. Eckey, A. Hoffmann, C. Thomsen, B. K. Meyer, H. Amano, I. Akasaki, T. Detchprohm, and K. Hira-

matsu, Appl. Phys. Lett. **68**, 1265 (1996).
[13] M. Tchounkeu, O. Briot, B. Gil, J. P. Alexis, and R. L. Aulombard, J. Appl. Phys. **80**, 5352 (1996).
[14] B. Gil, O. Briot, and R. L. Aulombard, Phys. Rev. B **52**, 17 028 (1995).
[15] S. Petit, D. Guennani, P. Gilliot, C. Hirlimann, B. Hönerlage, O. Briot, and R. L. Aulombard, Mater. Sci. Eng., B **43**, 196 (1997).
[16] H. Haag, P. Gilliot, R. Lévy, O. Briot, and R. L. Aulombard, MRS Internet J. Nitride Semicond. Res. **2**, Article 26 (1997).
[17] H. Haag, S. Petit, P. Gilliot, R. Lévy, O. Briot, and R. L. Aulombard, Mater. Sci. Eng., B **50**, 197 (1997).
[18] J. Eichler, P. Günter, and D. W. Pohl, *Laser Induced Gratings* (Springer, Berlin, 1979), Vol. 50.
[19] R. Tomasiunas, J. Moniatte, I. Pelant, P. Gilliot, and B. Hönerlage, Appl. Phys. Lett. **68**, 3296 (1996).
[20] R. Dingle, D. D. Sell, S. E. Stokowski, and M. Ilegems, Phys. Rev. B **4**, 1211 (1971).
[21] B. Hönerlage, R. Lévy, J. B. Grun, C. Klingshirn, and K. Bohnert, Phys. Rep. **124**, 161 (1985), and references cited therein.
[22] J. Valenta, J. Moniatte, P. Gilliot, B. Hönerlage, J. B. Grun, R. Lévy, and A. J. Ekimov, Phys. Rev. B **57**, 1774 (1998).
[23] M. Giehler, M. Ramsteiner, O. Brandt, H. Yang, and K. H. Ploog, Appl. Phys. Lett. **67**, 733 (1995).
[24] D. Kovalev, B. Averboukh, D. Volm, B. K. Meyer, H. Amano, and I. Akasaki, Phys. Rev. B **54**, 2518 (1996).
[25] R. Dingle and M. Ilegems, Solid State Commun. **9**, 175 (1971).
[26] C. Guénaud, E. Delporte, M. Voos, C. Delalande, B. Beaumont, M. Leroux, P. Gibart, and J. P. Faurie, MRS Internet J. Nitride Semicond. Res. **2**, Article 10 (1997).
[27] H. Haug and S. W. Koch, *Quantum Theory of the Optical and Electronic Properties of Semiconductors* (World Scientific, Singapore, 1990).
[28] C. Klingshirn, *Semiconductor Optics* (Springer, Berlin, 1995).
[29] J. Lagois, Phys. Rev. B **23**, 5511 (1981).
[30] W. Shan, B. D. Little, A. J. Fisher, J. J. Song, B. Goldenberg, W. G. Perry, M. D. Bremser, and R. F. Davis, Phys. Rev. B **54**, 16 369 (1996).
[31] R. Zimmermann, A. Eutener, J. Möbius, D. Weber, M. R. Hoffmann, W. W. Rühle, E. O. Göbel, B. K. Meyer, H. Amano, and I. Akasaki, Phys. Rev. B **56**, 12 722 (1997).
[32] Y. P. Varshni, Physica (Amsterdam) **34**, 149 (1967).
[33] D. S. Kim, J. Shah, J. E. Cunningham, T. C. Damen, W. Schäfer, M. Hartmann, and S. Schmitt-Rink, Phys. Rev. Lett. **68**, 1006 (1992).
[34] C. Klingshirn and H. Haug, Phys. Rep. **70**, 315 (1981).
[35] W. Shan, T. Schmidt, X. H. Yang, J. J. Song, and B. Goldenberg, J. Appl. Phys. **79**, 7 (1996); **79**, 3691 (1996).
[36] R. Seitz, C. Gaspar, T. Monteiro, E. Peira, M. Leroux, B. Beaumont, and P. Gibart, MRS Internet J. Nitride Semicond. Res. **2**, Article 36 (1997).
[37] V. Netiksis, B. Hönerlage, R. Weil, J. L. Loison, J. B. Grun, and R. Lévy, J. Appl. Phys. **74**, 5729 (1993).
[38] M. Benhmida, V. Netiksis, M. Robino, J. B. Grun, M. Pelant, M. Petrauskas, and B. Hönerlage, J. Appl. Phys. **80**, 8 (1996); **80**, 4632 (1996).
[39] A. Fejfar, I. Pelant, E. Sipek, J Kocha, G. Juska, T. Matsumoto, and Y. Kanemitsu, Appl. Phys. Lett. **66**, 1098 (1995).
[40] R. Klann, O. Brandt, H. Yang, H. T. Grahn, and K. H. Ploog, Appl. Phys. Lett. **70**, 1808 (1997).